Confocal Raman microspectroscopy reveals a convergence of the chemical composition in methanogenic archaea from a Siberian permafrost-affected soil

Paloma Serrano[1, 2], Antje Hermelink[3], Peter Lasch[3], Jean-Pierre de Vera[4], Nicole König[3], Oliver Burckhardt[1], Dirk Wagner[1#]

[1] GFZ German Research Centre for Geosciences, Helmholtz Centre Potsdam, Section Geomicrobiology, Telegrafenberg, 14473 Potsdam, Germany.

[2] Alfred Wegener Institute Helmholz Centre for Polar and Marine Research. Telegrafenberg A45 14473 Potsdam, Germany.

[3] Robert Koch Institute. Centre for Biological Threats and Special Pathogens; Nordufer 20 13353 Berlin, Germany.

[4] German Aerospace Center (DLR) Berlin, Institute of Planetary Research. Rutherfordstraße 2 12489 Berlin, Germany.

corresponding author: Dirk Wagner, GFZ German Research Centre for Geosciences, Helmholtz Centre Potsdam, Section Geomicrobiology, Telegrafenberg, 14473 Potsdam, Germany

Tel: +49 331 288 28800

Fax: +49 331 288 28802

Email: Dirk.Wagner@gfz-potsdam.de

Keywords: methanogenic archaea, Siberian permafrost, confocal Raman microspectroscopy, chemical composition, environmental adaptations, *mcrA*.

Running title: Chemical convergence in methanogens from Siberian permafrost

Abstract

Methanogenic archaea are widespread anaerobic microorganisms responsible for the production of biogenic methane. Several new species of psychrotolerant methanogenic archaea were recently isolated from a permafrost-affected soil in the Lena delta (Siberia, Russia), showing an exceptional resistance against desiccation, osmotic stress, low temperatures, starvation, UV and ionizing radiation when compared to methanogens from non-permafrost environments. To gain a deeper insight into the differences observed in their resistance, we described the chemical composition of methanogenic strains from permafrost and non-permafrost environments using confocal Raman microspectroscopy (CRM). CRM is a powerful tool for microbial identification and provides fingerprint-like information about the chemical composition of the cells. Our results show that the chemical composition of methanogens from permafrost-affected soils presents a high homology and is remarkably different from strains inhabiting non-permafrost environments. In addition, we performed a phylogenetic reconstruction of the studied strains based on the functional gene *mcrA* to prove the different evolutionary relationship of the permafrost strains. We conclude that the permafrost methanogenic strains show a convergent chemical composition regardless of their genotype. This fact is likely to be the consequence of a complex adaptive process to the Siberian permafrost environment and might be the reason underlying their resistant nature.

Introduction

Methanogenic archaea are strictly anaerobic microorganisms that belong to the phylum *Euryarchaeota* and produce methane as an obligate catabolic end-product (Ferry, 1993). About 85 % of the annual global methane formation is mediated by methanogenic archaea

(Thauer *et al.*, 2008). Once released, methane can either be oxidized in biotic and abiotic processes or accumulate in the Earth's atmosphere as a greenhouse gas, where it will slowly oxidize by means of photochemical reactions. The atmospheric methane concentration has increased more than twofold in the last 200 years (Hedderich & Whitman, 2006), contributing to the increase in the Earth's temperature over the last decades.

Terrestrial permafrost predominantly occurs in the northern hemisphere and covers approximately 24 % of Earth's land surface. It represents a significant natural source of methane, largely of biological origin (Fung *et al.*, 1991, Wagner *et al.*, 2003). Arctic tundra soils in Siberia are permanently frozen throughout the year with the exception of the thin active layer, subjected to seasonal freeze-thaw cycles with *in situ* temperatures ranging from -45°C to 25°C (Wagner *et al.*, 2005). Several novel strains of psychrotolerant methanogenic archaea were recently isolated from the active layer of a permafrost-affected soil in the Lena Delta (Siberia, Russia). Unlike psychrophiles, psychrotolerant methanogens show a broad adaptive potential to the fluctuating environmental conditions, including a wide temperature range and the subsequent geochemical gradients (Simankova *et al.*, 2003) as it can be observed in the active layer of the permafrost environment. Previous experiments in our labs have demonstrated the remarkable resistance of Siberian permafrost methanogenic strains against desiccation, osmotic stress, low temperatures and starvation when compared to methanogenic archaea from non-permafrost environments (Morozova & Wagner, 2007, Wagner *et al.*, 2013). They also exhibit a high level of resistance to monochromatic and polychromatic UV and ionizing radiation (D. Wagner, unpublished data), comparable to that of *Deinococcus radiodurans* (Brooks & Murray, 1981). In addition, methanogens from Siberian permafrost environments are able to survive simulated Martian thermo-physical conditions (Morozova *et al.*, 2007) and simulated Martian subsurface analog conditions (Schirmack *et al.*, 2013), in contrast to other psychrophilic methanogens from non-

permafrost habitats such as *Methanogenium frigidum* (Franzmann *et al.*, 1997) from Ace Lake, Antarctica, which cannot resist these conditions (Morozova *et al.*, 2007). Among the Siberian permafrost isolates, the genera *Methanosarcina* and *Methanobacterium* are broadly represented. *Methanosarcina* can metabolize a broad spectrum of substrates, including hydrogen, methanol and acetate (Liu & Whitman, 2008). *Methanobacterium* species present a hydrogenotrophic metabolism, growing on H_2+CO_2 or formate (Ferry, 1993).

The reasons why psychrotolerant methanogens from Siberian permafrost environments are more resistant to a broad range of extreme parameters than their relatives from psychrophilic and mesophilic non-permafrost habitats remains unknown. We hypothesize that this difference might depend on specific adaptations reflected in their biomolecules. In order to investigate the chemical composition of methanogens from Siberian permafrost and non-permafrost habitats, we used a Raman spectroscopy setup. Raman spectroscopy is a vibrational spectroscopic technique that provides fingerprint-like information about the overall chemical composition of the cell and requires a minimal sample preparation, allowing a rapid nondestructive investigation (Rösch *et al.*, 2005, Harz *et al.*, 2009). The strains in this study were previously investigated by Fourier-transformed Raman spectroscopy in an attempt to perform a bulk analysis of their chemical composition. However, due to the nature of the cells and the presence of metabolic byproducts (Serrano *et al.*, 2013), confocal Raman microspectroscopy (CRM) proved to be the optimal method. CRM combines a dispersive Raman setup with a high-numerical aperture confocal microscope, enabling the study of the chemical structure and composition of individual cells under diffraction-limited conditions (Krause *et al.*, 2008, Hermelink *et al.*, 2009). This technique has allowed the characterization of the chemotaxonomic features in multiple microorganisms to the species and even strain level (Maquelin *et al.*, 2002).

Additionally, a phylogenetic reconstruction based on the gene *mcrA* was performed to investigate the phylogenetic relationships among the strains in this study. Microbial phylogenetics is often based on the 16S rRNA molecule, although other important molecular markers for classification are known. In methanogenic archaea, the functional gene *mcrA* codes for the α subunit of the methyl coenzyme-M reductase (*MCR*), which catalyzes the last step of the methanogenesis (Ferry, 2010). MCR is thought to be unique to methanogens and, since it retains a common function, sequence comparisons are considered to provide valid phylogenetic data (Reeve, 1992). The gene *mcrA* has also proven to be an alternative to 16S rRNA in the phylogenetic analysis of methanogen populations (Luton *et al.*, 2002).

In this study, we describe the overall chemical composition of three strains of methanogens from Siberian permafrost and two strains of methanogens from non-permafrost habitats by means of CRM in an attempt to gain insights into their different resistance to extreme and fluctuating environmental parameters. In addition, we give a phylogenetic overview of the studied strains and their evolutionary relationship based on the functional gene *mcrA*. Finally, we discuss the differences in the chemical nature in relation to the reconstructed phylogeny.

Materials and Methods

Archaeal cultures

The three psychrotolerant methanogenic strains from Siberian permafrost environments used for this study were *Methanosarcina soligelidi* SMA-21 (Wagner *et al.*, 2013), SMA-17 and SMA-27. They were isolated from the active layer of permafrost-affected soils in the Lena Delta, Siberia (Russia). In nature, they thrive in temperatures ranging from -45ºC to +25ºC and even if they can grow at temperatures down to 0°C, the optimal growth temperature of

120 the isolates is 28ºC. *Ms. soligelidi* SMA-21 (DSM 26065^T) and SMA-17 appear as irregular
121 cocci, ~1µm in diameter and cell aggregation is often observed. They show 99.9 %
122 homology on the 16S rRNA sequence with *Methanosarcina mazei* (Mah, 1980). SMA-27
123 cells are elongated rods, ~3-4 µm long. Their closest relative according to the 16S rRNA
124 molecule is *Methanobacterium congolense (Cuzin et al., 2001) (*96.4 % homology. Wagner,
125 unpublished). Additionally, two mesophilic strains from non-permafrost habitats were used
126 as reference strains. *Ms. barkeri* DSM 8687 originates from a peat bog in northern Germany
127 (Maestrojuan *et al.*, 1992) and *Ms. mazei* DSM 2053 was isolated from a mesophilic sewage
128 sludge plant in California, USA. Both strains were obtained from the German Culture
129 Collection of Microorganisms and Cells (DSMZ, Braunschweig, Germany), appear as
130 irregular cocci, ~1µm in diameter, grow in colonies and are found in diverse environments.
131 Both show an empirical optimal growth at the temperature of 28ºC.
132
133 **Growth conditions of methanogenic strains**
134 For an accurate comparison of the spectra, the Raman measurements were performed in
135 living cells from pure cultures grown at optimal conditions at 28^{0}C and at their stationary
136 phase of growth (approximately 3 weeks after innoculating the cultures). The permafrost
137 strains were not grown at simulated permafrost conditions for the following reasons: 1)
138 permafrost conditions are extremely difficult to simulate, considering the yearly long term
139 freezing and thawing cycles, that consequently cause changes in the salinity and the
140 geochemical gradients, very difficult to accurately simulate in culture conditions. 2) The
141 freezing and thawing cycles that would partly recreate permafrost conditions would cause
142 environmental stress on the cells due to the changing parameters. Therefore, the permafrost
143 populations would contain less viable healthy cells and the quality of the cultures between
144 fresh non-permafrost cultures and aged permafrost cultures exposed to environmental stress
145 would not allow a fair comparison of the chemical composition.

Pure cultures were grown in sealed bottles that contained 50 mL of MW medium [(L^{-1}): NH_4Cl 0.25 G, $MgCl_2$ x $6H_20$, 0.4 G, $CaCl_2$ x $2H_2O$ 0.1 G, KCl, 0.5 G, KH_2PO_4, 0.2 G, Na HCO_3, 2.7 G, Cysteine, 0.3 G, Na_2S, 0.2 G; trace element solution (Balch *et al.*, 1979), 10mL; vitamin solution (Bryant *et al.*, 1971), 10mL] in *Methanosarcina* strains and CS medium [(L^{-1}): NH_4Cl, 0.3 G, $MgCl_2$ x $6H_2O$, 0.4 G, $CaCl_2$ x $2H_2O$, 0.16 G, NaCl, 1.0 G, KCl, 0.5 G, K_2HPO_4 0.25 G, Na HCO_3, 2.7 G, Na-Acetate, 0.25 G, $Na_2S_2O_4$, 0.1 G, Na_2S, 0.25 G; trace element solution (Imhoff-Stuckle & Pfennig, 1983), 1mL; vitamin solution (Bryant *et al.*, 1971), 1mL] in the case of SMA-27 (since the growth of SMA-27 in MW medium was suboptimal). Both media contain 2 mL resazurin (7-Hydroxy-3H-phenoxazin-3-on-10-oxide). The bottles were flushed and pressurized to one atmosphere with H_2/CO_2 (80:20 v/v). For sample preparation, 200 mL from four sets of pure cultures in the stationary phase of growth were centrifuged at 7900 g for 40 min and 4℃ and washed twice in 200 mL of distilled water at 4600 g for 30 min and 4℃. 7 µL of the cell suspensions were air-dried onto a CaF_2 slide, previously diluted 1:10 and 1:100 for a better observation of the single cells.

Raman microspectroscopy

Raman spectra were captured using a WITec (Ulm, Germany) Model alpha 300R confocal Raman microspectroscope (CRM), calibrated according to the manufacturer's instructions with an Ar/Hg spectral lamp. The CRM contained an ultra-high throughput spectrometer (UHTS300) and used a back-illuminated EMCCD camera (Andor Technology PLC, Belfast, Northern Ireland) as detector. All the measurements presented in this article were performed with an apochromatic Nikon E Plan (100x/0.95) objective (Tokyo, Japan) and a working distance of 0.230 mm at an excitation wavelength of 532 nm (frequency doubled Nd-YAG laser; 35mW laser power). A minimum of 20 individual cells were measured, each of them

171 with 5s of accumulation time under full pixel binning and without gaining at the camera.
172 Further technical details about the Raman equipment and measurements were reported in
173 detail in Serrano *et al.* (2014).

174 For hierarchical clustering of the CRM spectra, a cosmic ray removal procedure was first
175 performed on the spectra, followed by the individual export of each spectrum via an ASCII
176 interface into OPUS 5.5 (Bruker Optik GmbH, Rheinstetten, Germany). As part of the pre-
177 processing, we carried out a quality test in order to assess the signal-to-noise ratio and a pre-
178 selection of the cell-based spectra that contains the principal components of the spectrum.
179 The first derivative with Savitzky-Golay smoothing/ derivative filter was applied using 9
180 smoothing points and normalized vectors. Spectral distances between pairs of individual
181 spectra were obtained based on the data from the 796-1854 and 2746-3205 cm^{-1} spectral
182 regions as D-values (Naumann, 2000) derived from normalized Pearson's product
183 momentum correlation coefficient. The normalization allows a variation between D-value=0
184 (r=1: high correlated data/identity), D-value=1000 (r=0: uncorrelated data) and D-
185 value=2000 (r=-1:anti-correlated spectra) and prevents negative values (Helm *et al.*, 1991).
186 Average linkage was used as the clustering method. For the cluster analysis in Figure 4A, the
187 same method was applied to the average spectra obtained from averaging the individual
188 spectra of each strain shown in Fig. 2, including the outlying spectra.
189 The individual Raman intensities of all strains within the regions of 850 - 1850 and 2750 -
190 3200 cm^{-1} were treated as statistical variables and subjected to a rigid rotation via a Principal
191 Component Analysis (PCA) using the commercial software package MATLAB R2014a (The
192 Mathworks Inc, Natick, MA). This allows for the reduction of the original variables into
193 fewer, independent variables and to visualize and compare spectra between permafrost and
194 non-permafrost methanogenic strains.
195

196 **Phylogenetic analysis**

197 For phylogenetic analysis based on the *mcrA* sequence, the DNA was extracted from pure
198 cultures of the five mentioned strains following the user manual of the UltraClean® DNA
199 purification kit. The mcrA gene (Bokranz *et al.*, 1988) was amplified with the primers ME1
200 (forward: gCMATgCARATHggWATgTC) and ME2 (reverse:
201 TCATKgCTAgTTDggRTAgT). The PCR consisted in 32 cycles of 1min at 94ºC
202 (denaturation) followed by 1 min at 55ºC (annealing) and 1 min at 72ºC (elongation). A
203 previous denaturation stage (10min, 95ºC) and a final elongation (10min, 72ºC) were
204 performed, resulting in a 710 base pairs gene product. Sequencing was performed by GATC
205 Biotech (Constance, Germany). The consensus sequence was obtained using the software
206 CodonCode Aligner (Codoncode Cooperation, MA, USA). The nucleotide sequences from
207 the Siberian permafrost strains were uploaded in GeneBank under the numbers KJ432634
208 (*mcrA Ms. soligelidi* SMA-21), KJ432635 (*mcrA* SMA-17) and KJ432633 (*mcrA* SMA-27).

209 A multiple alignment of the five *mcrA* sequences was performed with ClustalW (Thompson
210 *et al.*, 1994) through Geneious pro 5.6.6 (Biomatters Ltd.) and a maximum likelihood tree
211 (1000 bootstraps) was built using the GTR substitution model including the methanogenic
212 archaea *Methanopyrus kandleri* (Kurr *et al.*, 1991) order *Methanopyrales*, (Genbank
213 U57340) as an outgroup.

214

215 **Results**

216 **Raman spectra of permafrost and non-permafrost methanogens**

217 The Raman spectra of the analyzed strains *Ms. soligelidi* SMA-21, SMA-17 and SMA-27
218 from Siberian permafrost and *Ms. barkeri* and *Ms. mazei* from non-permafrost habitats are
219 illustrated in Figure 1 and described Table 1. The highest Raman intensity in all spectra was

220 the CH_2 stretching vibration around 2936 cm^{-1}. The spectra from permafrost strains exhibited
221 a shoulder at 2885 cm^{-1}, which corresponds to the symmetric CH_3 stretching (Socrates,
222 2004), indicating significant differences in the aliphatic chain composition between
223 permafrost and non-permafrost methanogenic strains. Raman modes of proteins were found
224 at 1669 cm^{-1} (amide I) and at 1243-1275 cm^{-1} (region of amide III). Their intensities are
225 correlated and show slightly lower values for *Ms. soligelidi* SMA-21 and SMA-17. The peak
226 at 1610 cm^{-1} corresponds to the bond C=C found in aromatic amino acids phenylalanine and
227 tyrosine and reached higher intensities in non-permafrost strains, whereas the peak at 1589
228 cm^{-1} is associated to the ring breathing modes of ribonucleotides guanine and adenine as well
229 as the amino acid tryptophan and was absent in permafrost strains. The intensity of the 1460
230 cm^{-1} band, attributed to CH_2 deformation, was similar in all strains investigated. The peaks at
231 1344 cm^{-1} and 1338 cm^{-1} were both assigned to the deformation of the group CH in
232 carbohydrates and proteins (Ivleva *et al.*, 2009). The peak at 1344 cm^{-1} reached the highest
233 intensity for *Ms. mazei*, the lowest for *Ms. soligelidi* SMA-21 and SMA-17 and intermediate
234 values for SMA-27 and *Ms. barkeri,* whereas the one at 1338 cm^{-1} was unique to the
235 permafrost strains SMA-21 and SMA-17. All the mentioned bands varied slightly in
236 bandwidth, position and intensity for each strain. The peaks in the spectral region located
237 between 1200 and 800 cm^{-1} showed relative higher intensities in permafrost strains than in
238 non-permafrost strains, including the bands located at 1167 cm^{-1} (C-C and C-O ring
239 breathing), 1128 cm^{-1} (characteristic of the C-O-C in the glycosidic link) and 1054 cm^{-1} (C-O
240 and C-C from carbohydrates, and C-C and C-N in proteins, Neugebauer *et al.*, 2007). The
241 band at 1008 cm^{-1} was attributed to the symmetric benzene/ pyrrole in-phase and out-of-
242 phase breathing modes of phenylalanine (Ivleva *et al.*, 2009). The band at 860 cm^{-1}
243 corresponded to the C-C stretching modes and the C-O-C glycosidic link in polysaccharides
244 (Pereira *et al.*, 2004), and the peak at 835 cm^{-1} was exclusive to the permafrost strains and

245 was attributed to the ring breathing of the amino acid tyrosine and the group O-P-O present
246 in nucleic acids (Ivleva *et al.*, 2009).

247 The cluster analysis based on the Raman spectra showed the similarities and differences in
248 the overall chemical composition of permafrost and non-permafrost strains in stationary
249 phase, revealing two chemically different clusters illustrated in Figure 2 (individual spectra)
250 and 4A (average spectra). CRM spectra corresponding to individual cells of the same
251 microbial strain clustered together, with the exception of two spectra from SMA-27 and
252 three spectra from *Ms. soligelidi* SMA-21 (Fig. 2). The outlying spectra of SMA-27 were
253 equally distant to the spectra of the SMA-27 cluster and the *Ms. soligelidi* SMA-21/ SMA-17
254 cluster, separated by the distance of 104.6 and 123.1 D-value units, respectively. Three
255 outlying spectra of *Ms. soligelidi* SMA-21 were separated by 70.8 D-value units from the
256 *Ms. soligelidi* SMA-21/ SMA-17 cluster. Spectra from *Ms. mazei*, *Ms. barkeri* and SMA-17
257 cells were less heterogeneous and grouped into unique clusters at the strain level.

258 The cluster analysis in Figure 4A shows an overview of the phenotypic resemblance in the
259 chemical composition based on the average spectra of each strain, obtained from averaging
260 the individual spectra, including the outliers (and therefore disregarding the intraspecific
261 variances in the heterogeneity). Strains *Ms. soligelidi* SMA-21 and SMA-17 were most
262 similar, separated by 15.6 D-values. The cluster *Ms. soligelidi* SMA-21/ SMA-17 was
263 closely related to the strain SMA-27, also from Siberian permafrost, distanced by 37.8 D-
264 values. Apart from the permafrost group, the spectra from *Ms. mazei* and *Ms. barkeri* (non-
265 permafrost strains) grouped together, separated by 24.4 D-value units. The total distance
266 between the permafrost and the non-permafrost cluster was 84.4 D-values.

267 The PCA in Figure 3A shows the score plot of the first 3 principal components (PCs) that
268 cumulatively captured 88.04 % of the total variance in the spectral regions of interest. It
269 demonstrated that each strain occupies a distinct variable space, forming non-overlapping

data clouds. Additionally, PC1 can effectively separate the permafrost and the non-permafrost groups (note that PCA has been carried out on normalized spectra), illustrating shared spectral features within each of the two groups and divergent spectral features between these groups. Figure 3B shows the loadings of the first three PCs. PC1 (62.72% of the variance) is dominated by strong bands at the labeled wavelengths, which correspond to the vibrational modes of proteins, carbohydrates, nucleic acids and lipids (Neugebauer *et al.*, 2007, Ivleva *et al.*, 2009) and illustrate additional differences within the chemical composition between permafrost and non-permafrost strains. The downward peaks correspond to distinct features shared by non-permafrost methanogens, whereas the upward peaks correspond to shared features of permafrost methanogens.

Phylogenetic relationships of methanogenic archaea

A maximum likelihood tree (GTR substitution model, 1000 bootstraps) was built for the studied methanogens according to the *mcrA* nucleotide sequence, using *Methanopyrus kandleri* as the outgroup (Fig. 4B). All the *Methanosarcina* species clustered together, with *Ms. soligelidi* SMA-21 and SMA-17 from the Siberian permafrost showing identical *mcrA* sequences. The cluster *Ms. soligelidi* SMA-21/ SMA-17 was closely related to *Ms. mazei*, sharing a 98.5 % identity in their sequences. *Ms. mazei* and *Ms. barkeri* presented a 91.5 % homology. Finally, SMA-27 was the most evolutionary distant strain, sharing only 61% of the *mcrA* nucleotide sequence with the rest of the studied strains.

Discussion

Previous studies have shown that methanogenic archaea from permafrost habitats are more tolerant to different environmental stress factors compared to those from non-permafrost

areas (Morozova *et al.*, 2007, Morozova & Wagner, 2007, Morozova *et al*., 2015). In this study, we have shown that Siberian permafrost and non-permafrost strains could be classified into two different groups according to their chemical composition on the basis of CRM analysis. The Siberian permafrost strains *(Ms. soligelidi* SMA-21, SMA-27 and SMA-17) show a higher degree of similarity in their chemistry and the spectral clusters of SMA-27 and *Ms. soligelidi* SMA-21 present outlying spectra, suggesting that their populations are more chemically heterogeneous than the other strains (Fig. 2). However, the high phenotypic heterogeneity within a cell population and diversity between different growth phases described for *Ms. soligelidi* SMA-21 (*Serrano et al.*, (2014) were also observed in all the strains investigated in this study. When comparing the cluster analysis of the individual spectra (Fig. 2) with the average spectra (Fig. 4A), two puzzling facts concerning the scale, and therefore the heterogeneity, were observed: (i) The scales were different, despite referring to the same data; (ii) The heterogeneity within the SMA-27 population was larger than the overall distance in the average spectra. The explanation relies on the fact that the average spectra were obtained by averaging the single spectra from each strain, including the outliers, which considerably increased the variance of the corresponding strains (*Ms. soligelidi* SMA-21 and most remarkably SMA-27). The largely different variances within each strain were therefore not proportionally weighed for the cluster analysis of the average spectra and, despite this fact, the permafrost and the non-permafrost strains cluster in different groups according to their chemical composition.

The clusters resulting from the PCA of the individual spectra (Fig. 3A) support the cluster analysis in Figure 2, evidencing that CRM can be used to differentiate between strains, which form non-overlapping data clouds on the plot. Furthermore, the first principal component has separated out permafrost from non-permafrost strains. However, the Raman-spectroscopic differences between permafrost and non-permafrost strains (Fig. 1 and 3B) are

non-conclusive when it comes to pointing to specific biomolecules that differentiate the two groups. Raman spectroscopy exclusively shows the differences in the vibrational modes and thus in the chemical composition, without revealing the biomolecule itself. For example, the band at 2885 cm^{-1} (Fig. 1) corresponds to the symmetric CH_3 stretching, indicating significant differences in the aliphatic chain composition between permafrost and non-permafrost methanogens, but this technique does not allow for the identification of specific phospholipids.

On the other hand, the evolutionary relationships among the strains do not correspond in all cases with the topology found for the chemical composition. The phylogenetic relationship provided by the gene *mcrA* proves that the permafrost strains do not form a monophyletic group (Fig. 4B). The *mcrA* sequences of *Methanosarcina* strains from the Siberian permafrost (SMA-21 and SMA-17) are closely related to each other, whereas SMA-27 presents only 61% of homology with the rest of the strains and aligned with the genus *Methanobacterium*. Sequence alignments of the 16S rRNA molecule corroborate these findings (Wagner, unpublished), evidencing that SMA-27 forms a distantly-related sister group. The non-permafrost strains, *Ms. mazei* and *Ms. barkeri*, share a remarkable degree of homology in both chemical composition and genetic information. The maximum likelihood analysis based on *mcrA* shows a full bootstrap support for the node that separates *Ms. barkeri* (Fig. 4B). Although the other two nodes within that group are not completely resolved, it is evidenced that *Ms. mazei* is the most closely related strain to *Ms. soligelidi* SMA-21 and SMA-17.

This study proves that Siberian permafrost methanogenic strains share a related chemistry, regardless of their evolutionary origin. In other words, methanogens with different genotypes can exhibit an analogous phenotype in terms of chemical composition. This finding points to the evidence of the complexity of the adaptations to the environmental conditions,

suggesting that methanogenic strains from Siberian permafrost may have developed common biochemical adaptations to sub-zero temperatures, freeze-thaw cycles, osmotic stress and high levels of background radiation over geological time scales. A plausible phenomenon explaining the convergent chemical composition in permafrost strains despite their different genotype is the horizontal gene transfer (HGT) (Jain *et al.*, 1999). HGT allows the rapid incorporation of novel functions that provide a selective advantage to the organism and there is proof of HGT in the evolution of some genes coding for enzymes involved in methanogenic pathways (Fournier, 2009). The Alien Hunter programme (Vernikos & Parkhill, 2006) predicted that between 35% and 51% of the genome of methanogenic archaea has undergone HGT, and the highest percentage corresponded to the psychrophilic archaeon *Methanococcoides burtonii* (Allen et al., 2009). However, the gene *mcrA* chosen for this study is not affected by this phenomenon. All *mcr* operons appear to have evolved from a common ancestor and since MCR plays a key role in the methanogenesis, it is highly conserved and provides valid phylogenetic information, independent of the 16S rRNA information (Reeve, 1992). Despite this fact, other operational genes involved in perhaps anabolic pathways may have experienced HGT with the consequent production of molecules/metabolites that might have provided a selective phenotypic advantage to the cells. That selective advantage would enable them to survive in the Siberian permafrost environment and leading to a convergent chemical phenotype of the methanogenic archaea. The specific biomolecules that are different for permafrost and non-permafrost strains and may provide the selective advantage, however, cannot be discriminated by means of CRM.

CRM allows the discrimination between molecules based on their specific vibrational modes. When investigating the composition of a single cell, CRM can be used to describe only the Raman-active biomolecules such as molecules containing aromatic rings

368 (phenylalanine, tryptophan, pigments etc.), but this technology does not allow the
369 identification of specific biomolecules (e.g. a particular protein or carbohydrate).

370 Figure 1 and Table 1 illustrate both the quantitative (band intensities) and qualitative (band
371 position) chemical differences found between spectra of permafrost (psychrotolerant) and
372 non-permafrost (mesophilic) methanogens cultured at their optimal conditions and growth
373 temperature (28ºC). Some peaks experience a slight shift in comparison to their standard
374 value in the literature (e.g. the symmetric benzene/ pyrrole in-phase and out-of-phase
375 breathing modes of phenylalanine appear at 1008 cm^{-1} in contrast to Ivleva *et al.*, 2009, with
376 the same peak described at 1003cm^{-1}). Although the calibration of the spectrometer was
377 verified once a week, calibration errors of 3-5 wavenumber units (deviation of approximately
378 one pixel of the 1024 x 128 CCD element) cannot be excluded. However, a systematic
379 calibration error of the CRM measurements is expected to only exert a minor effect on the
380 results of cluster or principal component analysis. Furthermore, the Raman peaks illustrating
381 the differences between the permafrost and non-permafrost groups are not identical in Fig. 1
382 and Fig. 3B, although they are focused in the same major spectral regions. For instance, the
383 region 1571-1690 cm^{-1} in the average spectra (Fig.1) contains minor fluctuations that
384 correlate with the peaks identified on the PCA (Fig. 3B). This spectral region corresponds to
385 proteins (amide I, 1669cm^{-1}) and aromatic amino acids, and evidences differences between
386 permafrost and non-permafrost strains. The same fact is observed within the region 2846 -
387 2959 cm^{-1} (Fig. 1), which corresponds to lipids: multiple additional differences in the
388 vibrational modes of permafrost and non-permafrost methanogens are revealed within that
389 region on the PCA (Fig. 3B).

390 The underlying compositional differences might be correlated with convergent biochemical
391 adaptations to the Siberian permafrost environment and could explain the resistant nature of
392 the permafrost strains when compared to other non-permafrost methanogens. These

393 adaptations to the Siberian permafrost environment might be related to one or multiple
394 adaptive mechanisms to cold, radiation, desiccation, osmotic stress, and their corresponding
395 seasonal fluctuations. The adaptive mechanisms described for psychrotolerant methanogenic
396 archaea include modifications in cellular components and functional machinery or proteins
397 in order to maintain their structural flexibility and activity under cold temperatures and
398 changing conditions (Dong & Chen, 2012). For instance, the membrane lipids show
399 increasing levels of unsaturation of the fatty acids (Cavicchioli *et al.*, 2000). In Figure 1, the
400 peak at 2936 cm^{-1} (CH_2 stretching region) presents a similar intensity for all strains, pointing
401 to the fact that the lipid content is comparable. Next to it, the peak at 2885 cm^{-1} (symmetric
402 CH_3 stretching) reveals a noticeable contrast between permafrost and non-permafrost strains,
403 denoting qualitative differences in the aliphatic chain composition of the lipids (Socrates,
404 2004), even when growing at mesophilic temperatures. In addition, previous studies have
405 reported that proteins in psychryotolerant methanogens present a reduced hydrophobic core
406 and a less charged protein surface (Reed *et al.*, 2013), as well as cold-adaptive chaperone
407 proteins, such as Csp, CSD and TRAM domain proteins (Giaquinto *et al.*, 2007). This study
408 shows that the protein levels are slightly more abundant in non-permafrost strains and SMA-
409 27, according to the amide I (1669 cm^{-1}) and amide III bands (1275-1243 cm^{-1}), which
410 correspond to the peptide bond of proteins. On the other hand, the peak at 1610 cm^{-1} is
411 unique to phenylalanine and tyrosine and it is more abundant in non-permafrost strains.
412 However, the peak at 1008 cm^{-1}, assigned to phenylalanine, is slightly higher in the
413 permafrost methanogenic strains. The peaks at 1589 cm^{-1} and 835 cm^{-1} correspond also to
414 aromatic amino acids, but are not unique to them. These findings are in principle compatible
415 with the reduced hydrophobic cores of proteins in psychrotolerant methanogens found by
416 Reed *et al.* (2013), since the proteins from permafrost methanogenic strains present
417 relatively less aromatic (and hydrophobic) amino acids, with the exception of phenylalanine.
418 Unfortunately, only the aromatic amino acids tryptophan, tyrosine and phenylalanine

419 produce Raman scattering, and therefore this technique does not allow further amino acid
420 identification.

421 Particularly interesting is the band at 860 cm^{-1}, which is especially prominent in permafrost
422 strains and was previously assigned to the C-O-C 1,4-glycosidic link present in
423 carbohydrates and polysaccharides (Pereira *et al.*, 2004, Ivleva *et al.*, 2009). This distinctive
424 band together with the band at 1338 cm^{-1} confirms the presence of polysaccharide of similar
425 nature in permafrost strains. Many microorganisms, including archaea, have been reported to
426 produce exopolysaccharides (EPSs, sugar-based polymers that are secreted by
427 microorganisms to the surrounding environment) as a strategy to survive adverse conditions
428 (Poli *et al.*, 2011). In fact, they have been shown to play a protective role against desiccation
429 (Ophir & Gutnick, 1994), which might be the case of the permafrost methanogenic strains in
430 the perennially frozen ground or frozen period of the active layer.

431 In conclusion, this study presents proof of concept that distantly related methanogens
432 (*Methanosarcina* and *Methanobacterium)* occurring in the same habitat have independently
433 developed similarities in the chemical composition (Hoover & Pikuta, 2009). Extreme
434 conditions such as sub-zero temperatures and osmotic stress generally affect macromolecule
435 structures and the thermodynamics of chemical reactions, having the same impact on all
436 microorganisms. Hence, microorganisms that inhabit in the same extreme environment have
437 proven that the features and adaptations that unite them as a group are stronger than the
438 variation imposed by their phylogeny (Cavicchioli, 2006). The microbial communities of
439 permafrost environments have been often referred to as a "community of survivors"
440 (Friedmann, 1994) that have found themselves trapped in this environment and have
441 outcompeted those unable to withstand the given environmental conditions through a process
442 of continuous selection that lasted millions of years (Gilichinsky *et al.*, 1993). The Siberian

permafrost methanogenic strains in this study corroborate the convergence of a certain phenotype in response to the surrounding environment, independent of the genotype.

Acknowledgements

The authors acknowledge Christoph Liedtke (University of Basel) and Susanne Liebner (GFZ German Research Centre for Geosciences) for advice on phylogenetic reconstructions and Mashal Alawi (GFZ German Research Centre for Geosciences) for his comments on the manuscript. The authors declare no conflicts of interest. This work was supported by the Federal Ministry of Economics and Technology (BMWi) by a grant to DW (50WB1152).

References

Allen M, Lauro F, Williams T, *et al.* (2009) The genome sequence of the psychrophilic archaeon, Methanococcoides burtonii: the role of genome evolution in cold adaptation. *ISME Journal* **3**: 1012–1035.

Balch W, Fox G, Magrum L and Wolfe R. (1979) Methanogens: reevaluation of a unique biological group. *Microbiol Rev* **43**: 260-296.

Bokranz M, Baumner G, Allmansberger R, Ankel-Fuchs D and Klein A (1988) Cloning and characterization of the methyl coenzyme M reductase genes from Methanobacterium thermoautotrophicum. *J Bacteriol* **170**: 568-577.

Brooks BW & Murray RGE (1981) Nomenclature for "*Micrococcus radiodurans*" and other radiation-resistant cocci: Deinococcaceae fam. nov. and Deinococcus gen. nov., including five species. *Int J Syst Bacteriol* **31**: 353-360.

Bryant MP, Tzeng SF, Robinson JM & Joyner Jr. AE (1971) Nutrient requirements of methanogenic bacteria. *Adv Chem Ser* **105**: 23-40.

Cavicchioli R (2006) Cold-adapted archaea. *Nature Rev Microbiol* **4**: 331-343.

Cavicchioli R, Thomas T & Curmi PMG (2000) Cold stress response in Archaea. *Extremophiles : life under extreme conditions* **4**: 321-331.

Cuzin N, Ouattara AS, Labat M & Garcia J (2001) *Methanobacterium congolense* sp. nov., from a methanogenic fermentation of cassava peel. *Int J Syst Evol Microbiol* **51**: 489 - 493.

Dong X & Chen Z (2012) Psychrotolerant methanogenic archaea: diversity and cold adaptation mechanisms. *Science China Life Science* **55**: 415-421.

Ferry JG (1993) *Methanogenesis. ecology, physiology, biochemistry and genetics*. Chapman and Hall, New York, London.

Ferry JG (2010) The chemical biology of methanogenesis. *Planet Space Sci* **58**: 1775-1783.

Fournier G (2009) Horizontal gene transfer and the evolution of methanogenic pathways. *Horizontal gene transfer: genomes in flux (*Gogarten, M.B. ; Gogarten, J.P. ; Olendzenski, L., eds.), pp. 163-179. Humana Press.

480 Franzmann PD, Liu Y, Balkwill DL, Aldrich HC, Conway de Macairo W & Boone DR (1997)
481 *Methanogenium frigidum* sp. nov., a psychrophilic, H_2-using methanogen from Ace Lake,
482 Antarctica. *Int J Syst Bacteriol* **47**: 1068-1072.
483 Friedmann EI (1994) Permafrost as microbial habitat. *Viable microorganisms in Permafrost.*
484 (Gilichinsky DA, ed.) pp. 21-26. Russian Academy of Science, Pushchino.
485 Fung I, John J, Lerner J, Matthews E, Prather M, Steele LP & Fraser PJ (1991) Three-dimensional
486 model synthesis of the global methane cycle. *J Geophysical Res* **96**: 13033-13065.
487 Giaquinto L, Curmi PMG & Siddiqui KS (2007) Structure and function of cold shock proteins in
488 Archaea. *J Bacteriol* **189**: 5738–5748.
489 Gilichinsky DA, Soina VS & Petrova MA (1993) Cryoprotective properties of water in the Earth
490 cryolithosphere and its role in exobiology. *Origins Life Evol Biosphere* **23**: 65 - 75.
491 Harz M, Rösch P & Popp J (2009) Vibrational spectroscopy- a powerful tool for the rapid
492 identification of microbial cells at the single-cell level. *Cytometry Part A* **75A**: 104-113.
493 Hedderich R & Whitman W (2006) *Physiology and biochemistry of methane-producing archaea*.
494 Springer Verlag, New York.
495 Helm D, Labischinski H & Naumann D (1991) Elaboration of a procedure for identification of
496 bacteria using Fourier-transform infrared spectral libraries: A stepwise correlation approach.
497 *J Microbiol Methods* **14**: 127-147.
498 Hermelink A, Brauer A, Lasch P & Naumann D (2009) Phenotypic heterogeneity within
499 microbial populations at the single-cell level investigated by confocal Raman
500 microspectroscopy. *Analyst* **134**: 1149–1153.
501 Hoover RB & Pikuta EV (2009) Psychrophilic and psychrotolerant microbial extremophiles in
502 polar environments. *Polar microbiology* (Bej AK, Aislabie J & Atlas R, eds.), pp. 115 -156.CRC
503 Press.
504 Imhoff-Stuckle D & Pfennig N (1983) Isolation and characterization of a nicotinic acid-
505 degrading sulfate-reducing bacterium, *Desulfococcus niacini* sp. nov. *Arch Microbiol* **136**: 194–
506 198.
507 Ivleva NP, Wagner M, Horn H, Niessner R & Haisch C (2009) Towards a nondestructive
508 chemical characterization of biofilm matrix by Raman microscopy. *Anal Bioanal Chem* **393**:
509 197-206.
510 Jain R, Rivera MC & Lake JA (1999) Horizontal gene transfer among genomes: The complexity
511 hypothesis. *PNAS* **96**: 3801–3806.
512 Krause M, Rösch P, Radt B & Popp J (2008) Localizing and identifying living bacteria in an
513 abiotic environment by a combination of Raman and fluorescence microscopy. *Anal Chem* **80**:
514 8568–8575.
515 Kurr M, Huber R, König H, Jannasch HW, Fricke H, Trineone A, Kristjansson JK & Stetter KO
516 (1991) *Methanopyrus kandleri*, gen. and sp. nov. represents a novel group of
517 hyperthermophilic methanogens, growing at 110°C. *Arch Microbiol* **156**: 239-247.
518 Liu Y & Whitman W (2008) Metabolic, phylogenetic, and ecological diversity of the
519 methanogenic archaea. *Ann NY Acad Sci* **1125**: 171-189.
520 Luton PE, Wayme JM, Sharp RJ & Riley PW (2002) The mcrA gene as an alternative to 16S rRNA
521 in the phylogenetic analysis of populations in landfill. *Microbiol* **148**: 3521-3530.
522 Maestrojuan GM, Bonne JE, Mah RA, Menaia JAGF, Sachis MS & Boone DR (1992) Taxonomy and
523 halotolerance of mesophilic Methanosarcina strains, assignment of strains to species, and
524 synonymy of *Methanosarcina mazei* and *Methanosarcina frisia*. *Int J Syst Bacteriol* **42**: 561-
525 567.
526 Mah RA (1980) Isolation and characterization of of *Methanococcus mazei*. *Current Microbiology*
527 **3**: 321- 326.
528 Maquelin K, Choo-Smith L-P, Kirschner C, Ngo Thi NA, Naumann D & Puppels GJ (2002)
529 Vibrational spectroscopic studies of microorganisms. *Handbook of vibrational spectroscopy,*
530 (Chalmers JM & Griffiths PR, eds.), pp. 3308 - 3334. John Wiley, Chichester.
531 Morozova D & Wagner D (2007) Stress response of methanogenic archaea from Siberian
532 permafrost compared with methanogens from non permafrost habitats. *FEMS Microbiol Ecol*
533 **61** 16–25.

534 Morozova D, Möhlmann D & Wagner D (2007) Survival of methanogenic archaea from Siberian
535 permafrost under simulated martian thermal conditions. *Orig Life Evol Biosph* **37**: 189–200.
536 Morozova D, Moeller R, Rettberg P & Wagner D (2015) Enhanced radiation resistance of
537 *Methanosarcina soligelidi* SMA-21, a new methanogenic archaeon isolated from a Siberian
538 permafrost-affected soil in direct comparison to *Methanosarcina barkeri*. *Astrobiology* **15**:
539 Naumann D (2000) Infrared spectroscopy in microbiology. *Encyclopedia of Analytical*
540 *Chemistry: applications, theory and instrumentation.* (Meyers R., ed), pp. 102-131. John Wiley
541 and Sons Ltd, Chichester.
542 Neugebauer U, Schmid U, Baumann K, Zieburh W, Kozitskaya S, Deckert V, Schmitt M & Popp J
543 (2007) Towards a detailed understanding of bacterial metabolism- spectroscopic
544 characterization of *Staphylococcus epidermidis*. *Chem Phys Chem* **8**: 124-137.
545 Ophir T & Gutnick D (1994) A role for exopolysaccharides in the protection of microorganisms
546 for dessication. *Appl Environ Microbiol* **60**: 740-745.
547 Pereira R, Martin AA, Tierra-Criollo CJ & Santos I (2004) Diagnosis of squamous cell carcinoma
548 of human skin by Raman spectroscopy. *Proceedings of SPIE* **5326**: 106 - 112.
549 Poli A, Di Donato P, Abbamondi GR & Nicolaus B (2011) Synthesis, production, and
550 biotechnological applications of exopolysaccharides and polyhydroxyalkanoates by archaea.
551 *Archaea* **2011**: 1-13.
552 Reed CJ, Lewis H, Trejo E, Winston V & Evilia C (2013) Protein adaptations in archaeal
553 extremophiles. *Archaea* **2013**: 273-275.
554 Reeve JN (1992) Molecular biology of methanogens. *Annu Rev Microbiol* **46**: 165-191.
555 Rösch P, Harz M, Schmitt M*, et al.* (2005) Chemotaxonomic identification of single bacteria by
556 micro-Raman spectroscopy: application to clean-room-relevant biological contaminations.
557 *Appl Environ Microbiol* **71**: 1626–1637.
558 Schirmack J, Böhm M, Brauer C, Löhmannsröben HG, de Vera JP, Möhlmann D & Wagner D
559 (2013) Laser spectroscopic real time measurements of methanogenic activity under
560 simulated Martian subsurface analog conditions. *Planetary and Space Science* **98**:198-204
561 Serrano P, Wagner D, Böttger U, de Vera JP, Lasch P & Hermelink A (2014) Single-cell analysis
562 of the methanogenic archaeon *Methanosarcina soligelidi* from Siberian permafrost by means
563 of confocal Raman microspectroscopy for astrobiological research. *Planet Space Sci* **98**: 191-
564 197.
565 Simankova MV, Kotsyurbenko OR, Lueders T, Nozhevnikova AN, Wagner B, Conrad R &
566 Friedrich MW (2003) Isolation and characterization of new strains of methanogens from cold
567 terrestrial habitats. *Syst Appl Microbiol* **26**: 312-128.
568 Socrates G (2004) Alkane group residues: CH group. *Infrared and Raman characteristic group*
569 *frequencies Tables and charts.* (Socrates G., ed.), pp. 50-67. John Wiley and sons Ltd.,
570 Chichester.
571 Thauer RK, Kaster AK & Seedorf H (2008) Methanogenic archaea: ecologically relevant
572 differences in energy conservation. *Nat Rev Microbiol* **6**: 579-591.
573 The MathWorks, Inc. MATLAB and Statistics Toolbox Release 2014a. Natick, Massachusetts.
574 Thompson JD, Higgins DG & Gibson TJ (1994) CLUSTAL W: improving the sensitivity of
575 progressive multiple sequence alignment through sequence weighting, position specific gap
576 penalties and weight matrix choice. *Nucleic Acids Res* **22**: 4673 - 4380.
577 Vernikos GS & Parkhill J (2006) Interpolated variable order motifs for identification of
578 horizontally acquired DNA: revisiting the Salmonella pathogenicity islands. *Bioinformatics* **22**:
579 2196-2203.
580 Wagner D, Kobabe S, Pfeiffer E-M & Hubberten H-W (2003) Microbial controls on permafrost
581 fluxes from a polygonal tundra of the Lena Delta, Siberia. *Permafrost Periglac Process* **14**: 173-
582 185.
583 Wagner D, Lipski A, Embacher A & Gattinger A (2005) Methane fluxes in permafrost habitats of
584 the Lena Delta: effects of microbial community structure and organic matter quality.
585 *Environmental Microbiology* **7**: 1582-1592.

586 Wagner D, Schirmack J, Ganzert L, Morozova D & Mangelsdorf K (2013) *Methanosarcina*
587 *soligelidi* sp. nov., a desiccation and freeze-thaw resistant methanogenic archaeon isolated
588 from a Siberian permafrost-affected soil. *Int J Syst Evol Microbiol* **63**: 2986-2991.

589

590 **Table 1.** Description of the Raman bands identified in the spectra of the methanogenic
591 strains from Siberian permafrost (*Ms. soligelidi* SMA-21, SMA-17 and SMA-27) and the
592 mesophilic methanogens (*Ms. mazei* and *Ms. barkeri)* measured with an excitation
593 wavelenght of 532nm. The values of the bands exclusive to one or a few strains are
594 presented in grey. + indicates the presence of a certain band, and - its absence. Qualitative
595 differences are indicated with the symbol (+), meaning a higher intensity of the peak and
596 therefore cellular abundance.

597

Wavenumber (cm^{-1})	Description	Ms. mazei	Ms. barkeri	SMA-17	Ms. soligelidi SMA-21	SMA-27
2936	CH_3 str and CH_2 str	+	+	+	+	+
2885	CH_3 str sym	-	-	+	+(+)	+(+)
1669	amide I (C=O str, NH_2 bend, C=N str)	+(+)	+(+)	+	+	+(+)
1610	C=C (Phe, Tyr)	+ (+)	+ (+)	+	+	+
1589	G + A ring str (nucleic acids); Trp	+	+	-	-	-
1460	δ(CH2) scis, CH2 def	+	+	+	+	+
1344	δ(CH)	+(+)	+(+)	+	+	+(+)
1338	δ(CH)	-	-	+	+	-
1275-1243	Amide III	+(+)	+(+)	+	+	+(+)
1167	C–C, C–O ring breath, asym	+	+	+	+	+
1128	C–C str, C–O–C glycosidic link; ring breath, sym (carbohydrates); C–N, C–C str (proteins); C–C str (lipids)	+	+	+	+	+

1054	C–O, C–C str (carbohydrates); C–C; C–N (proteins)	+	+	+(+)	+(+)	+(+)
1008	n(CC) aromatic ring (Phe)	+	+	+(+)	+(+)	+(+)
860	C-C str; C-O-C glycosidic link	+	+	+(+)	+ (+)	+(+)
835	Ring breath Tyr; O–P–O str (DNA/RNA)	-	-	+	+	+

598

599

Figure Legends

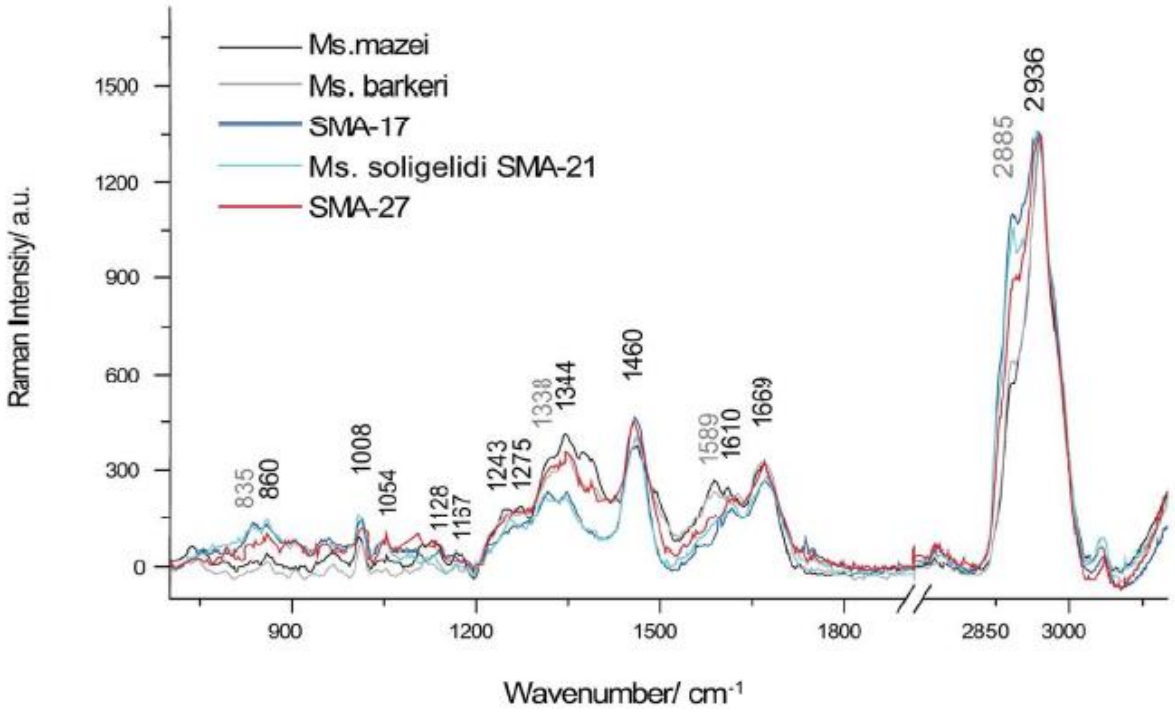

Figure 1. Average Raman spectra of methanogenic strains from Siberian permafrost (*Ms. soligelidi* SMA-21, SMA-17 and SMA-27) and non-permafrost environments (*Ms. mazei* and *Ms. barkeri)* measured with an excitation wavelength of 532nm. Note that values corresponding to the band positions specific to one or a few strains are presented in grey.

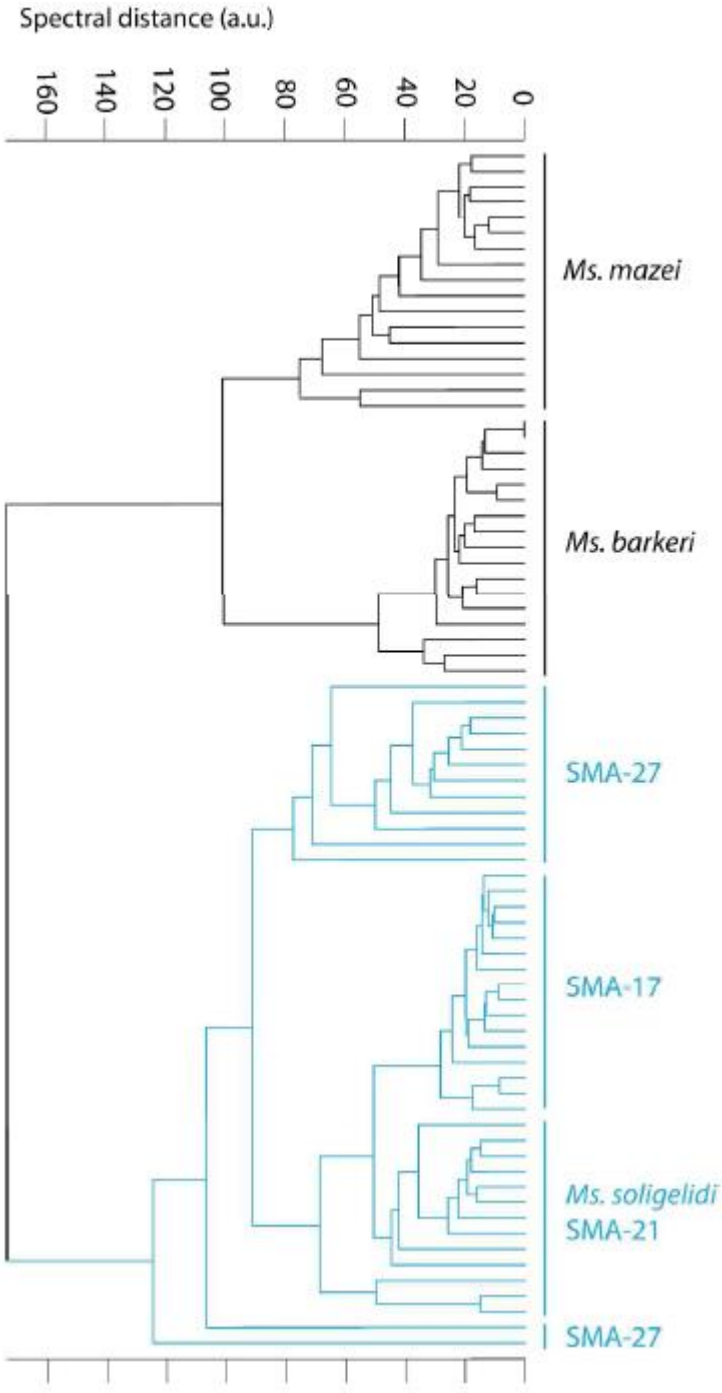

608
609 **Figure 2.** Cluster analysis (average linkage method) of Raman spectra from individual cells
610 from permafrost and non-permafrost strains in stationary phase. CRM spectra from
611 *Methanosarcina mazei* and *Ms. barkeri* (non-permafrost strains) form a cluster, which is well
612 separated from the cluster of permafrost strains (SMA-27, *Ms. soligelidi* SMA-21 and SMA-
613 17).

614

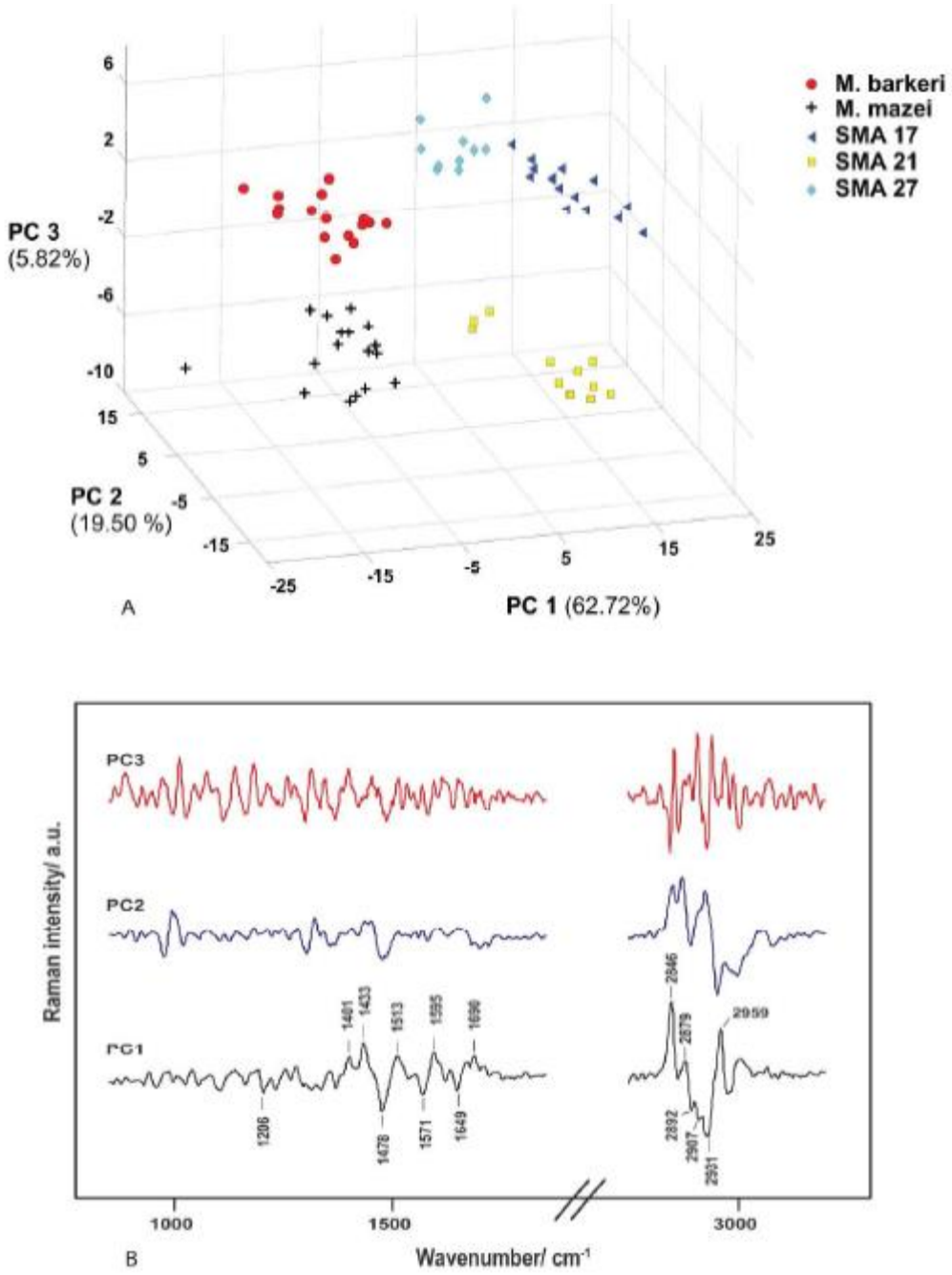

615
616 **Figure 3.** Principal Component Analysis (PCA) of the individual spectra of the five
617 methanogenic strains (A) Score plot of the first 3 principal components (PCs) of the total
618 variance of the spectra. (B) Loadings of the first three principal components, illustrating the
619 major spectral differences in PC1 (labeled peaks).

620

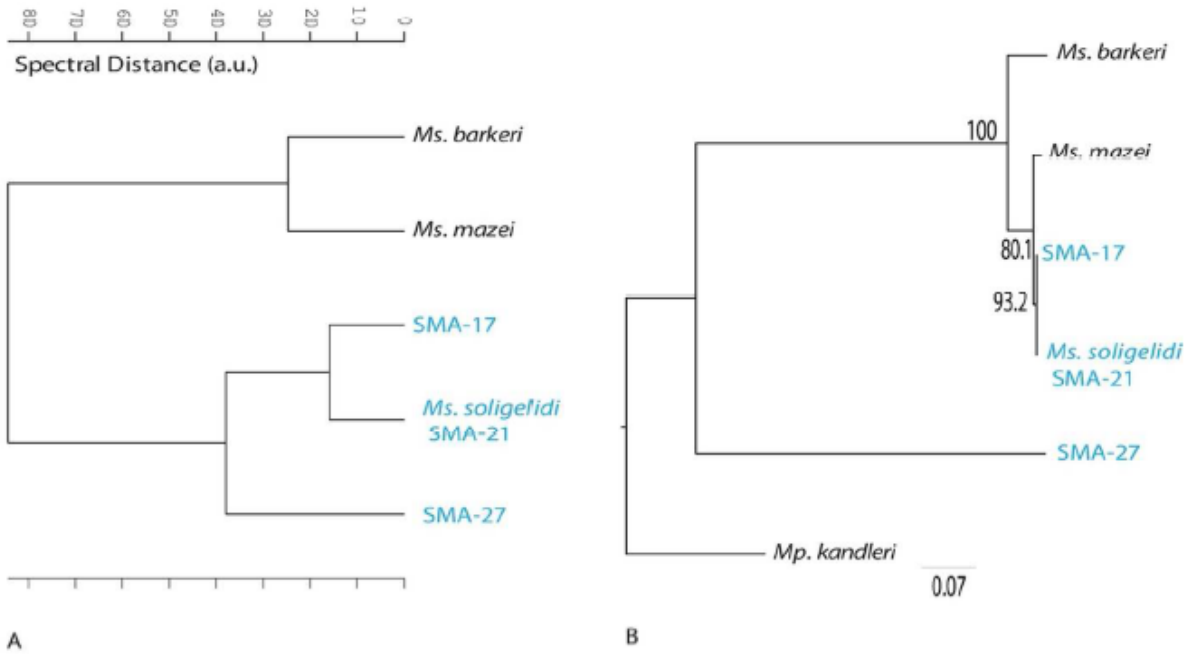

621
622 **Figure 4.** Chemical *vs*. phylogenetic relationships of methanogenic archaea from Siberian
623 permafrost *Methanosarcina soligelidi* SMA-21, SMA-17 and SMA-27 (in blue) and the two
624 non-permafrost strains used as reference *Ms. barkeri* and *Ms. mazei* (A) Cluster analysis of
625 the average Raman spectra from permafrost and non-permafrost strains in stationary phase
626 using the average linkage clustering method. (B) Maximum likelihood tree (GTR
627 substitution model, 1000 bootstraps) according to the mcrA nucleotide sequence.
628 *Methanopyrus kandleri* (*Methanopyrales*) was used as the outgroup. The branch support
629 values indicated in the nodes show the robustness of the phylogenetic reconstruction.

630